

Improved mechanical performance: Shear behaviour of strain-hardening cement-based composites (SHCC)

Gideon P.A.G. van Zijl *

*Division for Structural Engineering, University of Stellenbosch, South Africa
Faculty of Architecture, Delft University of Technology, The Netherlands*

Received 29 September 2006; accepted 16 April 2007

Abstract

The retardation of moisture and gas ingress associated with important degradation mechanisms in cement-based composites in general and reinforced concrete or prestressed concrete in particular is an ongoing research focus internationally. A dense outer layer is generally accepted to significantly enhance durability of structural concrete. However, cracking leads to enhanced ingress, unless the cracks are restricted to small widths. Strain-hardening cement-based composites (SHCC) make use of fibres to bridge cracks, whereby they are controlled to small widths over a large tensile deformation range. In this paper, SHCC shear behaviour is studied, verifying that the cracks which arise in pure shear are also controlled to small widths in these materials. The design of an Iosipescu shear test setup and specific SHCC geometry is reported, as well as the results of a test series. A computational model for SHCC, based on finite element theory and continuum damage mechanics, is elaborated and shown to capture the shear behaviour of SHCC. © 2007 Elsevier Ltd. All rights reserved.

Keywords: Shear properties; Fibre reinforcement; Mechanical properties; Microcracking

1. Cement-based materials development for structural durability

It is well known that moisture and gas ingress are major deradation processes in reinforced concrete, the dominating structural material internationally. Intense research efforts aim to quantify durability indexes in terms of resistance to chloride, water and oxygen penetration into concrete. Ingress retardation may lead to a major enhancement of structural life, or reduced life cycle cost. A significant research focus is on the virgin material durability. Enhanced durability is obtained in terms of dense matrices, for which waste materials like fly ash and ground granulated slagment have been shown to be beneficial. However, cracking of cement-based materials used to manufacture structures is unavoidable even in normal service conditions, calling for additional measures to ensure structural durability. Significant changes in moisture and gas migration processes when cracks arise lead to strongly increased ingress rates. Cracks in cement-based materials cannot be avoided and the need to

control structural durability through crack width limitation is well known and provided for in several design codes. Nevertheless, a sharp reduction in service free life of Civil Engineering Infrastructure and indeed a strong increase in the proportional expenditure on repair [1] are evident internationally. Appropriate detailing of steel reinforcement may distribute and control crack widths in concrete in many instances. However, the scale of cracking, and thereby also the ingress rates, can be reduced by orders of magnitude by designing materials for inherent crack control. Such a class of materials has been developed recently, namely pseudo strain-hardening cement-based composites (SHCC), in which cracks are bridged effectively by fibres to allow subsequent crack initiation at close spacing, at higher structural resistance. Through this process, multiple fine cracks arise in the cement-based matrix, whereby ingress rates of moisture are significantly reduced [2,3]. The application of SHCC is believed to hold significant potential for structural durability enhancement, or life cycle cost reduction of Civil Engineering Industry. Already, several authors, e.g. [4,5], have reported that these materials may benefit from the same waste stream ingredients (fly ash, slagment) used successfully in concrete to enhance durability.

* Tel.: +27 21 808 4498; fax: +27 21 808 4947.

E-mail address: gvanzijl@sun.ac.za.

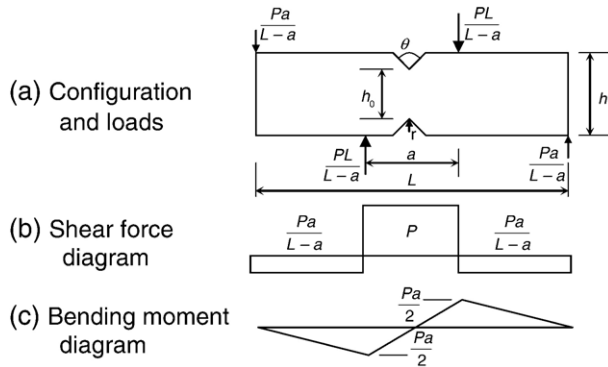


Fig. 1. Iosipescu specimen geometry, shear test lay-out and internal forces.

A particular class of highly ductile, strain-hardening, engineered cementitious composites (ECC), has been developed over the past decade. Through the ECC concept, it has become possible to design fibre-reinforced cement-based composites which have extreme tensile and flexural deformability and toughness, despite relatively low fibre volumes. In ECC the crack control is extended to high levels of tensile deformation [6,7]. Research towards linking SHCC strain level with crack width and stability, as well as with ingress rates of moisture and gas is ongoing [1]. These modern fibre-reinforced cement-based materials have the potential of significantly enhancing structural durability and will in the near future contribute immensely towards reduced life cycle cost of Civil Engineering Infrastructure. To realise this achievement on the short-medium term, a balance should be found between practical application, which drives awareness and research demand, and in-

depth fundamental research, including both physical and theoretical modelling to develop thorough understanding and allow derivation of rational design guidelines and rules. For the former, life cycle cost analysis is essential to convince Civil Engineering practice of the long-term benefits in sustainability. This paper contributes towards the latter, namely experimental and computational modelling to characterise the shear behaviour of ECC. An appropriate Iosipescu shear specimen geometry is designed through numerical analysis, to enable objective characterisation of shear behaviour.

2. Shear behaviour of ECC

Significant research effort has gone into characterisation of the tensile and flexural response of ECC, as well as ECC reinforced with steel bars (R/ECC). However, in addition to these qualities, the exploitation of the high, ductile shear resistance of these materials holds particular potential in reducing or avoiding the requirement of shear steel reinforcing in structural elements, or increasing energy absorption in shear for instance in seismic events, while maintaining crack control. Also for the use of ECC as repair layer or retrofitting material, or as thin layers in composite structural elements it is essential that the ductility and crack control is retained under shear load.

Shear response characterisation of ECC has received relatively little attention. Li et al. [8] executed Ohno shear beam tests of various cement-based composites, including plain concrete, reinforced concrete (RC) and a particular ECC containing high modulus polyethylene fibres. The results indicated

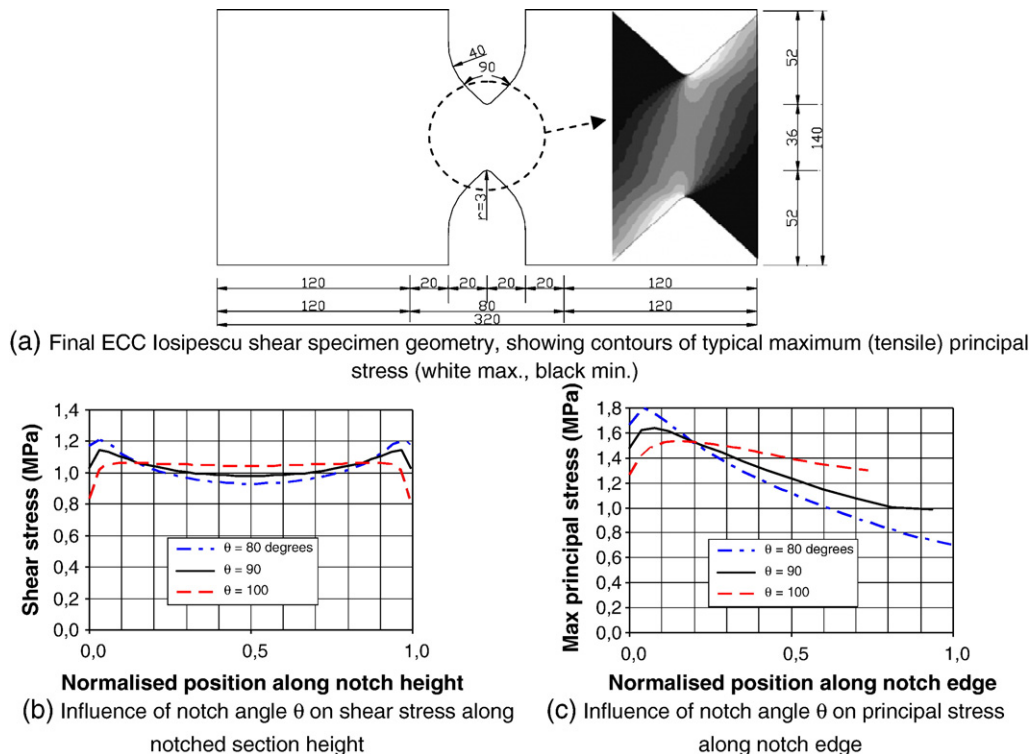


Fig. 2. FE refinement of Iosipescu specimen geometry (all dimensions in mm). (a) Final ECC Iosipescu shear specimen geometry, showing contours of typical maximum (tensile) principal stress (white max., black min.). (b) Influence of notch angle θ on shear stress along notched section height. (c) Influence of notch angle θ on shear stress along notch edge.

Table 1
ECC mix ingredients and proportions by mass

	Cement	Fly ash	GGCS	Water	Sand	V_f (%)	No. of specimens		
							CH ¹	SG ²	LVD ³
S1	0.5	0.45	0.05	0.4	0.5	0	3		
S2	0.5	0.45	0.05	0.4	0.5	1	3		
S3	0.5	0.45	0.05	0.4	0.5	2	3	3	3
S4	0.5	0.45	0.05	0.4	0.5	2.5	3	3	3

CH¹ Only Cross-Head measurement of deformation.

SG² Strain Gauge ($\pm 45^\circ$) measurement of deformation in notch area.

LVD³ Diagonal (45°) LVD³ measurement of deformation in notch area.

superior shearing ductility of ECC to that of RC. For both concrete and ECC an average shear strength approximately equal to the tensile strength was reported. However, in the Ohno beam a strongly nonuniform (parabolic) shear stress distribution complicates characterisation of shear strength. By introduction of a v-shaped notch (see Fig. 1), the Iosipescu shear beam [9] reduces the risk of failure in bending. In addition, by a choice of an appropriate notch geometry, an approximately uniform shear stress distribution is introduced in the notch section.

In the research project reported here, an appropriate Iosipescu beam geometry for ECC was refined through finite element analysis (FE), as shown in Fig. 2. Through a parametric study (notch angle, radius) a compromise between shear stress uniformity (Fig. 2(b)) and the proximity of the location of maximum

principal stress to the notch area is made by selecting a notch angle of 90° . This forces the crack initiation to be in the notch area, where a condition of pure shear exists, while maintaining a reasonably uniform shear stress distribution in the notch cross-section. Hereby, objective characterisation of shear response in the linear, as well as nonlinear, post-cracking response is enabled.

3. Experimental testing of shear response

A series of tests were performed on ECC materials of mix ingredients and proportions given in Table 1, mixed in an 8 liter capacity Hobart 3-speed mixer, cured in water at a constant 23°C and tested at the age of 14 days. A material testing machine was used under crosshead displacement control, set to 1.5 mm/min. In Fig. 3 the shear test setup is shown schematically, as well as the shear deformation measurement with either strain gauges (type KFG-10-120-d17-11) or an LVDT (type HBM WA/10) placed diagonally at 45° . The shear results shown in Fig. 4 indicate that failure is restricted to the notch area for SHCC. The position of crack initiation is indicated in the figure with the symbol “A”, confirming the position of maximum principal stress predicted by finite element analysis in Fig. 2(a). In the fibre-reinforced specimens these cracks are arrested. Subsequently, diagonal failure occurs for specimens with sub-critical fibre volume ($V_f < 2\%$), but for the specimens with $V_f \geq 2\%$, multiple cracks arise in the notch zone, indicating inherent shear crack control.

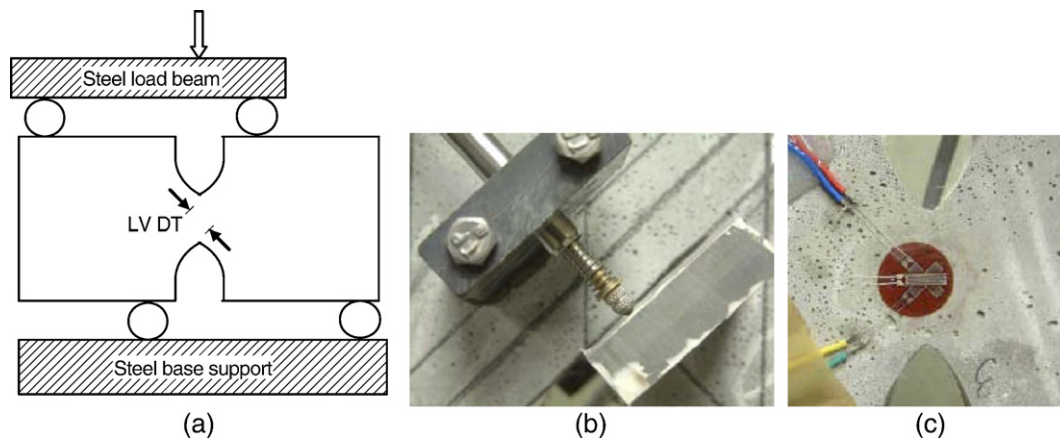


Fig. 3. (a) Iosipescu shear test, showing the (b) LVDT and (c) strain gauge measurement.

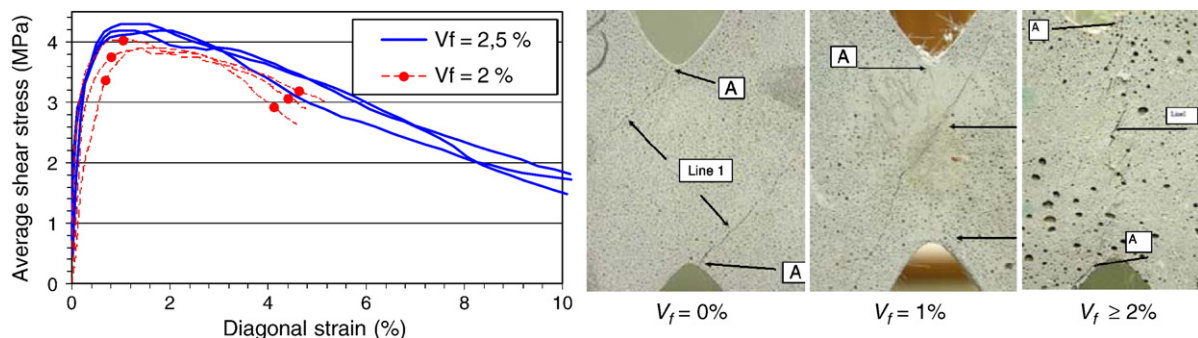


Fig. 4. Shear response of ECC Iosipescu specimens.

Table 2
Iosipescu average tensile and shear results (stress in N/mm², cov shown in brackets)

V_f	Shear response		Tensile response			
	Ultimate stress (τ_u)	G-modulus	First crack stress	Ultimate stress (σ_u)	Ultimate strain (ϵ_{tu} , %)	E-modulus
2.0%	3.99 (1%)	2800 (8%)	1.77 (13%)	2.68 (6%)	3.31 (38%)	7400 (14%)
2.5%	4.07 (2%)	3160 (7%)	1.85 (9%)	2.92 (7%)	4.55 (11%)	8500 (16%)

The deformation shown in Fig. 4 was measured with the LVDT placed diagonally (at 45°) over a gauge length of 25 mm. The elastic shear modulus was determined from the specimens instrumented with strain gauges in the notch section. A summary of the results is given in Table 2. Tensile properties are also reported in Table 2. These properties were obtained from separate tests on dogbone specimens of the exact same respective mixes. The test setup and specimen geometry are shown in Fig. 5. The average tensile stresses versus average tensile strain responses for the tensile specimens are shown in Fig. 6.

Note that the summarized results in Table 2 should be evaluated in the light of the small number of specimens per test. For reliable design guideline purposes, a larger data base of experimental results must be generated. From the statistical evaluation of the limited results in Table 2, it appears that the coefficient of variation (cov) for the shear properties, both in terms of strength and stiffness, is low, indicating a reliable material response. However, the coefficients of variation of the tensile E -modulus and the ultimate tensile strain are relatively large. An explanation of the smaller cov in shear than that in uniaxial tension may be the stabilizing orthogonal compression in the shear, or biaxial tension compression.

4. Computational analysis of shear response

To study the enhanced shear strength, computed from the results in Table 2 to be in the range $1.4 \leq \tau_u/\sigma_u \leq 1.5$ a computational model recently developed was used to study the Iosipescu shear test with the specimen geometry shown in Fig. 2. The model is based in standard computational continuum isotropic damage, which entails degradation of the elastic modulus matrix (\mathbf{D}^e) governed by damage evolution expressed in terms of a parameter w , which varies between 0 (no damage)

and 1 (complete damage). Hereby the relation between stress and strain is given as follows:

$$\sigma = (1 - w)\mathbf{D}^e \epsilon \quad (1)$$

In this paper plane stress is considered, with the stress and strain vectors defined as $\sigma = [\sigma_x \sigma_y \tau_{xy}]^T$ and $\epsilon = [\epsilon_x \epsilon_y \epsilon_{xy}]^T$ respectively. The damage evolves when a threshold strain ($\tilde{\epsilon}_0$) has been exceeded, expressed in one dimension for simplicity as

$$w = 1 - \frac{\sigma(\tilde{\epsilon} - \tilde{\epsilon}_0)}{E\tilde{\epsilon}} \quad (2)$$

To account for general stress states, an equivalent strain ($\tilde{\epsilon}$) is defined, which governs the damage evolution. For cement-based materials a formulation based on the maximum principal strain (ϵ_1) is commonly considered as follows:

$$\tilde{\epsilon} = \epsilon_1 = \frac{\epsilon_x + \epsilon_y}{2} + \sqrt{\left(\frac{\epsilon_x - \epsilon_y}{2}\right)^2 + \epsilon_{xy}^2} \quad (3)$$

However, this formulation can be shown analytically to predict diagonal tensile strength lower than the tensile strength [10], as depicted in Fig. 7(a). Instead, a novel equivalent strain definition is used here, defined as:

$$\tilde{\epsilon} = \frac{\epsilon_1 + \nu \epsilon_2}{1 - \nu^2} \quad (4)$$

with ν the Poisson's ratio and ϵ_2 the minimum principal strain defined as follows:

$$\epsilon_2 = \frac{\epsilon_x + \epsilon_y}{2} - \sqrt{\left(\frac{\epsilon_x - \epsilon_y}{2}\right)^2 + \epsilon_{xy}^2} \quad (5)$$

By using the equivalent strain defined in Eq. (4) an equal strength in tension and shear is obtained, Fig. 7(b). Note that a

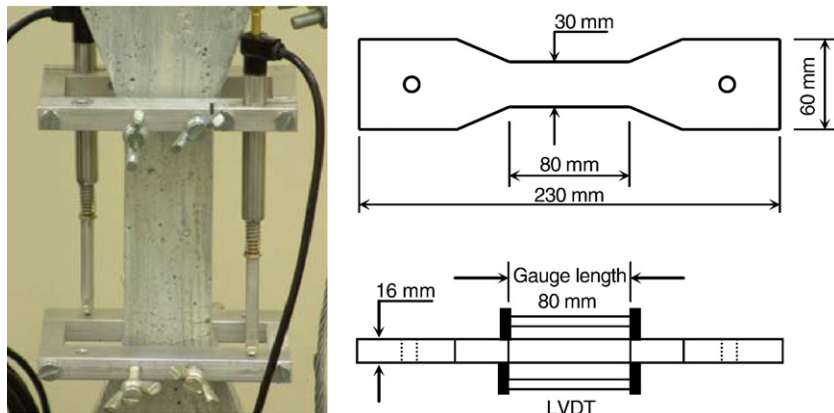


Fig. 5. Tensile test setup and dogbone specimen.

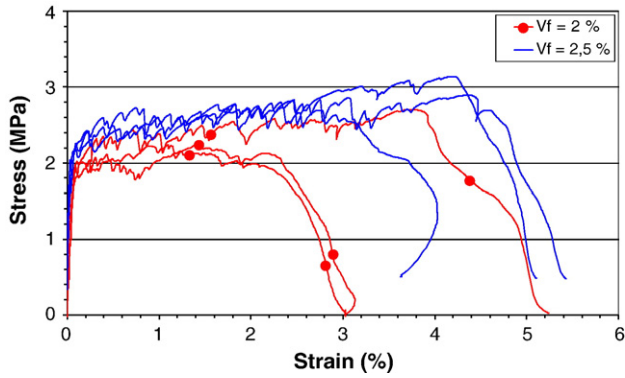


Fig. 6. Tensile test results for S3 and S4 type specimens.

trilinear stress–strain material law has been adopted as a simple simulation of (i) the linear-elastic branch, (ii) the subsequent strain-hardening branch and (iii) the final softening branch of the tensile response, as is clear in Fig. 7. By substituting simple expressions for the linear hardening and softening responses into Eq. (4), appropriate damage evolution expressions are obtained for ECC [10].

With this model, the average shear stress response shown in Fig. 8 is obtained for ECC specimens with $V_f = 2.5\%$. Clearly,

the shear strength is significantly underestimated by this choice of constitutive modelling. For comparison, the uniaxial tensile test responses of dogbone specimens, used for calibration of the model, are also shown in Fig. 8. The numerical ultimate shear strength reflects the diagonal tensile resistance, in agreement with Fig. 7(b), while the increased ductility in shear is captured reasonably, also in agreement with Fig. 7(b).

The contours of maximum principal strain are also shown in Fig. 8. These numerical results confirm the experimental observation that the two initial fine cracks that arise from the notch upper and lower edges respectively are arrested, after which multiple diagonal cracks arise centrally in the notch.

These numerical shear results indicate that the higher resistance in shear than in tension found experimentally for ECC is not due to the Iosipescu boundary value problem, because this is simulated by the FE model. Instead, a different failure mechanism acts in pure shear.

5. Discussion of shear response

In Fig. 9 equivalent stress states in the notch section are shown schematically, namely the vertical shear stress state and the equivalent biaxial tension compression principal stress state. This is used to postulate that the increased shear resistance is

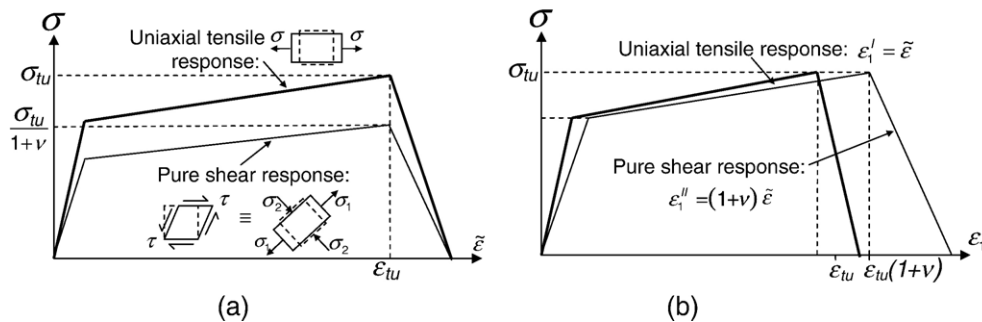


Fig. 7. Tensile and pure shear responses for (a) $\tilde{\varepsilon} = \varepsilon_1$ and (b) $\tilde{\varepsilon} = \frac{\varepsilon_1 + \nu\varepsilon_2}{1 - \nu^2}$.

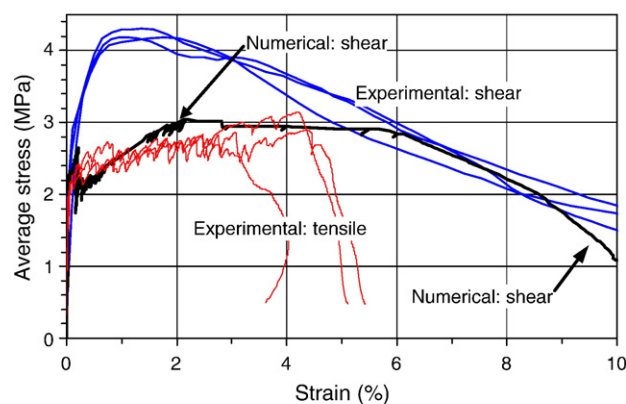
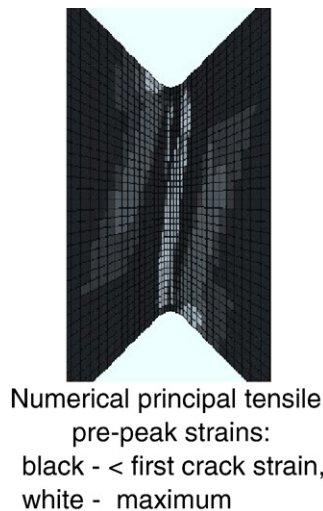


Fig. 8. Experimental and numerical shear response, compared with uniaxial tensile response of dogbone specimens.

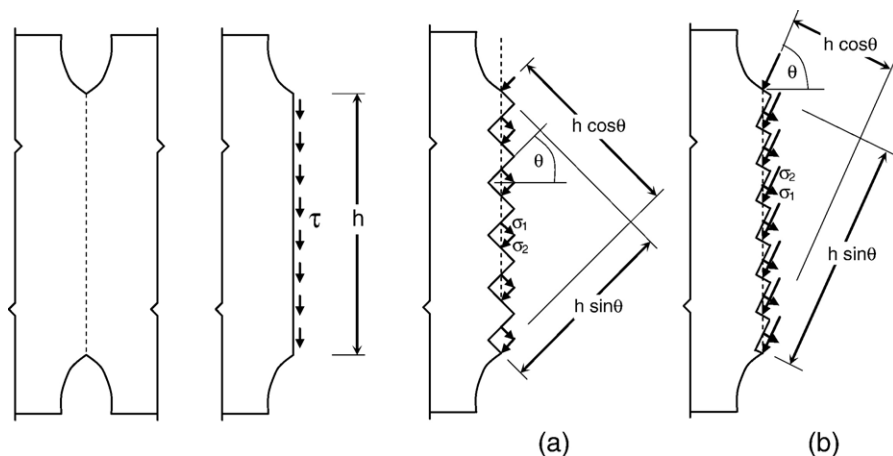


Fig. 9. Schematic representation of principal stresses in the failure plane at (a) first crack formation and (b) failure.

due to the tensile ductility. After crack initiation, which is represented by the equal tensile and compressive principal stress ($\pm 45^\circ$) state in Fig. 9(a), the tensile resistance can be maintained and increased due to effective crack bridging by fibres. Having not reached the compressive limit, the compressive principle stress can increase. This situation is shown in Fig. 9(b). This is accompanied by the multiple crack formation at increased diagonal tensile strain. By comparing the equivalent stress states, as represented by the Mohr circle in Fig. 10, it is clear that an increased shear resistance after initial crack formation can be mobilised. Note that this Iosipescu test purposefully prevents combined shear-flexure failure, which may lead to lower overall resistance if a shear crack propagates into the flexural zone and links with a flexural crack. For objectivity in prediction tools development and design guideline formulation, it is imperative that these different failure mechanisms are distinguished and characterised separately.

6. Conclusions

Motivated by the potential of SHCC in application for structural durability, this paper reports the study of pure shear behaviour of ECC. By the use of a specifically designed Iosipescu shear beam geometry for SHCC, multiple crack formation in ECC under pure shear has been demonstrated, underlying the potential

durability these materials may afford Civil Engineering Infrastructure, if used appropriately.

The shear strength of ECC has been shown to exceed its direct tensile strength by up to 50%, in agreement with the findings of Li et al. [8]. A mechanism of this increased resistance has been argued to be the ability of ECC to maintain its tensile resistance well beyond its first cracking strain, allowing principal stress rotation and accompanied increased orthogonal compression upon shear load increase. Of significant importance for improved structural durability and reliability is the observed immense ductility of ECC in diagonal tension, or shear. Crack width and spacing measurement and monitoring with sufficient resolution and accuracy are in process at the time of the submission of this manuscript. This behaviour is captured by the computational model presented. Refinement of the shear model awaits results of biaxial testing of ECC.

Acknowledgements

The support of the South African Ministry of Trade and Industry through the Technology and Human Resources for Industry Programme (THRIP), as well as the industrial partners of the THRIP project 2660 is gratefully acknowledged.

References

- [1] F.H. Wittmann, G.P.A.G. van Zijl, RILEM TC HFC, Subcommittee 2: Durability of SHCC. Conclusions of meetings and discussions during the HPFRCC workshop, in: G. Fischer, V.C. Li (Eds.), High Performance Fiber Reinforced Cementitious Composites (HPFRCC) in Structural Applications, RILEM Pro049 (2006) 109–114.
- [2] K. Wang, D.C. Jansen, S. Shah, A.F. Karr, Permeability study of cracked concrete, *Cement and Concrete Research* 27 (3) (1997) 381–393.
- [3] M. Lepech, V.C. Li, Water permeability of cracked cementitious composites, CD-Rom Proc. ICF, 2005, p. 4539, paper.
- [4] Gao Song, G.P.A.G. van Zijl, Tailoring ECC for commercial application, in: M. di Prisco, R. Felicetti, G.A. Plizzari (Eds.), Fibre-Reinforced Concretes (BEFIB'2004), RILEM Pro039 (2004) 1391–1400.
- [5] S. Wang, V.C. Li, Polyvinyl alcohol fiber reinforced engineered cementitious composites: material design and performances, in: G. Fischer, V.C. Li (Eds.), High Performance Fiber Reinforced Cementitious

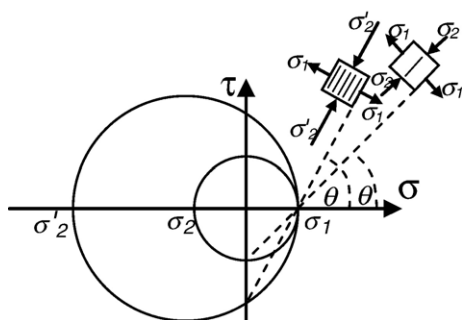


Fig. 10. Schematic Mohr circle indicating increased shear resistance beyond first crack.

- Composites (HPFRCC) in Structural Applications, RILEM Pro049 (2006) 65–73.
- [6] V.C. Li, S. Wang, C. Wu, Tensile strain-hardening behaviour of polyvinyl alcohol engineered cementitious composites (PVA-ECC), *ACI Materials Journal* (Nov-Dec 2001) 483–492.
- [7] M.B. Weimann, V.C. Li, Hygral behavior of engineered cementitious composites (ECC), *International Journal for Restoration of Buildings and Monuments* 9 (5) (2003) 513–534.
- [8] V.C. Li, D.K. Mishra, A.E. Naaman, J.K. Wigh, J.M. LaFave, H.C. Wu, Y. Inada, On the shear behavior of engineered cementitious composites, *Journal of Advanced Cement Based Materials* 1 (3) (1994) 142–149.
- [9] N. Iosipescu, New accurate method for single shear testing of metals, *Journal of Materials* 2 (3) (1967) 537–566.
- [10] W.P. Boshoff, G.P.A.G. van Zijl, A computational model for strain-hardening fibre-reinforced cement-based composites, *Journal of South African Institution of Civil Engineers (SAICE)* (2007) (in print).